RAPID COMMUNICATIONS

PHYSICAL REVIEW B VOLUME 42, NUMBER 7 1 SEPTEMBER 1990

Nonlinear electrodynamics in granular $YBa_2Cu_3O_7$: Measurements and models of complex permeability

Q. H. Lam, Y. Kim, and C. D. Jeffries

Physics Department, University of California, Berkeley, California 94720

and Materials and Chemical Sciences Division, Lawrence Berkeley Laboratory, Berkeley, California 94720

(Received 6 June 1990)

Measurements in ac and dc magnetic fields on a sintered rod of $YBa_2Cu_3O_7$ at 77 K yield a clear distinction between inter- and intragranular contributions to the complex harmonic permeability $\tilde{\mu}_n = \mu'_n - i\mu''_n$: two peaks in $\mu''_1(H_{ac})$ are clearly observed. These data, together with harmonic-power $P_n(H_{dc})$ measurements, are found to be well explained by a modified critical-state model, which, for fields $\lesssim 50$ Oe, is dominated by intergranular critical currents $J_c(H) \sim H_{loc}^{-2}$, a steeper field dependence than the original Bean-Anderson-Kim model.

High-temperature granular superconductors have a complex microstructure, and bulk specimens are generally supposed to consist of superconducting grains connected via weak links, referred to as intra- and intergranular components, respectively. Experimental evidence for this viewpoint has come from such experiments as anomalous ac magnetic susceptibility χ_{ac} at low fields,[1,2] limited transport critical current density J_c,[3] nonresonant microwave absorption,[4] and harmonic generation.[5-8] In our earlier papers[5,6] we proposed a zero-order model for harmonic generation based on an ensemble of superconducting current loops or Josephson junctions, which approximately explained our data for *powdered* $YBa_2Cu_3O_7$, but did not include loss mechanisms or fluxon dynamics, known to be significant. Müller *et al.*[8,9] and Ji *et al.*[10] pointed out that harmonic generation and χ_{ac} in *sintered* cylinders can be understood from the early and insightful phenomenological model of Bean,[11] as extended by Anderson and Kim[12] ("BAK" model). Here we report experimental data on harmonic generation and χ_{ac} in large ac fields for a cylinder of $YBa_2Cu_3O_7$, showing direct evidence for simultaneous existence of inter- and intragranular supercurrents.[13] A modified critical-state model is presented, which includes a stronger field dependence $J_c(H)$ than the BAK model and which is in quantitative agreement with all of our data for the intergranular component and also with detailed measurement of χ_{ac} by Kim *et al.*[14]

Experimental procedures. As previously described,[5,6] a sintered polycrystalline $YBa_2Cu_3O_7$ cylindrical rod ($\sim 3\times 20$ mm^2) is closely wound with a copper wire "receiver" coil and subject to coaxial applied uniform magnetic fields $H_a(t) = H_{dc} + H_1\cos(\omega t) + H_{scan}(t)$ from copper coils, all immersed in liquid N_2 in a magnetically shielded Dewar. The receiver coil (area A, $N = 135$ turns) generates a signal voltage $V_n(t)$ proportional to the time derivative of the spatially averaged instantaneous induction field in the sample $\bar{B}(t)$, which is expanded in a Fourier series to give the signal voltage (Gaussian units)

$$V_n(t) = [NAH_1\omega/c]\mu_{eff}\sum_{n=1}^{\infty}[n\mu'_n\sin(n\omega t) - n\mu''_n\cos(n\omega t)], \quad (1)$$

where the bracketed term is the signal amplitude without the sample, μ_{eff} is a geometrical filling factor, and the Fourier components are the real and imaginary parts of a complex ac permeability $\tilde{\mu}_n = \mu'_n - i\mu''_n$ for the nth harmonic; they are related to the ac susceptibility $\tilde{\chi}_n = \chi'_n - i\chi''_n$ by $\tilde{\mu}_1 = 1 + 4\pi\tilde{\chi}_1$, and $\tilde{\mu}_n = 4\pi\tilde{\chi}_n$ for all $n > 1$. Equation (1) is used to express, respectively, the separate contributions of the intergranular permeability $\tilde{\mu}$, and the intragranular permeability $\tilde{\mu}_g$, to the total signal voltage, which is studied by two methods.

(i) For $n = 1$, the sine and cosine signal components, V'_1 and V''_1, are separately measured by a lock-in detector. In Fig. 1, we plot $\mu'_1 \propto (V'_1/H_1)$ and $\mu''_1 \propto (V''_1/H_1)$ vs $\log_{10}H_1$. These plots are crucial to our interpretations

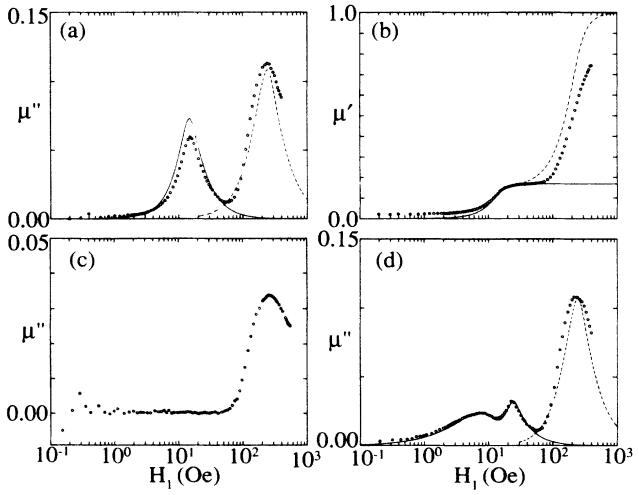

FIG. 1. (a),(b) Open circles: measured (Gaussian units) $\tilde{\mu}_{tot}$ vs H_1 for $YBa_2Cu_3O_7$ sintered rod (sample No. 2), $H_{dc} = 0$, $T = 77$ K, $f = 85$ Hz. Solid line: modified critical-state model predictions with $\beta = 1.8$ and $H_0 = 3$ Oe for intergranular component $\tilde{\mu}$. Dashed line: model calculation for intragranular component $\tilde{\mu}_g$ (reduced by a factor of 3 for μ''_g) using parameters $\beta_g = 1.0$, $H_{0g} = 5$ Oe, $\bar{R}_g = 10$ μm. (c) Measured μ''_{tot} vs H_1 for powdered $YBa_2Cu_3O_7$ (sample No. 4), $H_{dc} = 0$, $T = 77$ K, $f = 85$ Hz. The intergranular component is absent [cf. (a)]. (d) Same as (a) but with $H_{dc} = 10.2$ Oe.

since they show, quite directly, the distinct inter- and intragranular components.

(ii) For $n=2,\ldots,10$, the power spectrum $P_n \propto H_1^2 n^2[(\mu_n')^2+(\mu_n'')^2]$ is recorded by an analog spectrum analyzer (HP3585A) and plotted versus H_{dc}, as in Figs. 2(a) and 2(c), using the periodic slow field scan $H_{scan}(t)$. All data presented in the paper were made using the same sintered batch of $YBa_2Cu_3O_7$ (Ref. 15), cooled by immersion in liquid N_2 with $H_a=0$.

Modified critical-state model. Following the two-dimensional (2D) model of Clem[16] we assume a long bulk cylinder sample of radius R, containing long superconducting grains of radius R_g and penetration depth λ_g; the remaining volume is considered to be the intergranular regions, e.g., the barrier regions of Josephson junctions between grains, with penetration depth λ_J. We typically consider $R_g > \lambda_g$ and $\lambda_J \gg \lambda_g$ to get an effective medium model. A parallel field $H_a(t, r=R) = H_{dc} + H_1 \cos(\omega t)$ is applied at the surface. For $H_a > H_{c1J} \sim 1$ Oe, it is energetically favorable for vortices to enter the intergranular space, and form an array, resulting in a nearly uniform intergranular local magnetic field $H(r)$ to a depth dependent on the maximum (i.e., critical) transport current density J_c that the sample can support, which we assume to have the general form (Gaussian units)

$$J_c(H) = \alpha' \frac{c}{(|H|+H_0)^{\beta}}, \tag{2}$$

where α', H_0, and β are parameters to be determined by the data. Here $\alpha(H) \equiv \alpha'/(|H|+H_0)^{\beta-1}$ is the vortex pinning force density introduced by Anderson and Kim,[12] who assumed $\beta=1$. Bean's simplifying assumption[11] that the sample shielding current density J would be either zero in regions which have not yet been exposed to magnetic flux, or else $\pm J_c(H)$ in regions which have been subjected to an electromotive force induced by the motion of flux vortices, leads to the critical-state equation

$$\frac{dH}{dr} = \pm \frac{4\pi}{c} J_c(H). \tag{3}$$

Equations (2) and (3) are solved to find $H(r)$, and with $H_a(t)$, to find $H(r,t)$, $0<r<R$, $0<t<2\pi/\omega$. From this we calculate an analytical expression for the spatial average induction field in the sample

$$\bar{B}(t) = \mu_{eff}(\pi R^2)^{-1} \int_0^R H(r,t) 2\pi r\, dr .$$

From a discrete time series ($N=2048$) of the time derivative of this expression we used a fast Fourier transform to compute the Fourier components μ_n' and μ_n'' in Eq. (1) as functions of the experimentally known parameters (H_{dc}, H_1, R) and of those to be fitted by the data (α', H_0, β). However, the model yields a relationship

$$\alpha' = [(H_0+H^*)^{\beta+1} - H_0^{\beta+1}]/[4\pi(\beta+1)R],$$

where H^* is the external field value at which the flux front just reaches $r=0$; this corresponds to a maximum of $\mu''(H_1)$ at $H_1 \cong H^*$ which is readily measured experimentally, leaving only two independent parameters, β and H_0, to be selected by fitting the computed $\tilde{\mu}$ to the data for the intergranular component. For sufficiently large H_a the intergranular space becomes fully penetrated by vortices and $\mu' \to \mu_{eff}$, $\mu'' \to 0$. For still larger fields, $H_a \gtrsim H_{c1g}$, vortices penetrate the grains, and a similar and separate calculation is made to compute $\tilde{\mu}_g$ for the intragranular regions, using a different set of parameters μ_{effg}, R_g, α_g', H_{0g}, β_g. For experiments reported here it is a good approximation to take the total permeability $\tilde{\mu}_{tot} = \tilde{\mu} + \tilde{\mu}_g$.

Results and interpretation. One of our objectives is unambiguous experimental evidence for the existence of both inter- and intragranular contributions to $\tilde{\mu}_{tot}$, and to measure the corresponding critical currents $J_c(H)$ without resorting to the difficulties of assumed temperature dependences, which complicate the interpretation of χ_{ac} versus temperature data.[2,17,18] This is achieved in Fig. 1(a), measured values of μ_1'' vs $\log_{10} H_1$ over a wide range $0.1 < H_1 \lesssim 400$ Oe at $f=85$ Hz, $T=77$ K, $H_{dc}=0$. According to the above model $\mu''(H_1)$ shows a peak when

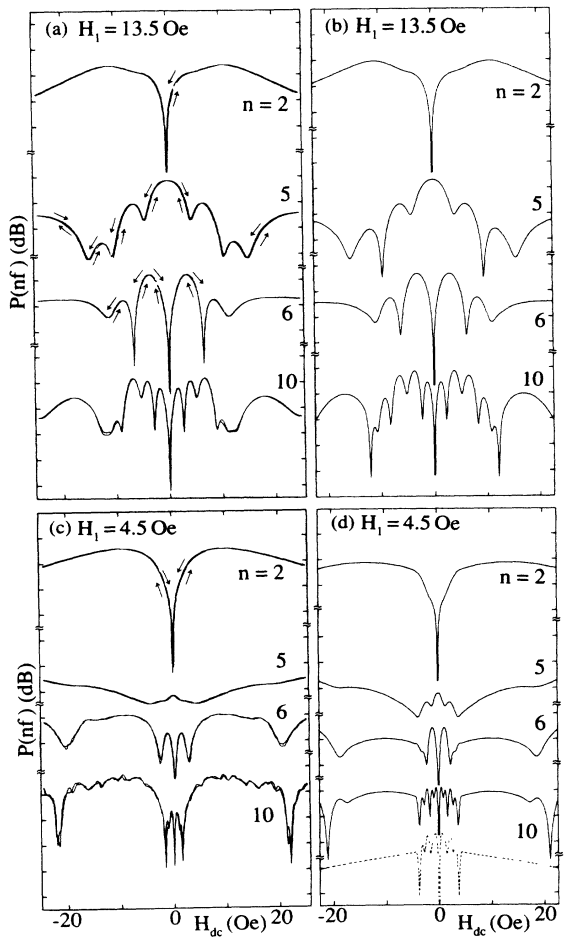

FIG. 2. (a) Measured harmonic power $P(nf)$ vs H_{dc} for $YBa_2Cu_3O_7$ sintered rod (sample No. 1). $T=77$ K, $H_1=13.5$ Oe, and $f=10.5$ kHz. Vertical scale division equals 10 dB. (b) Modified critical-state model predictions with $\beta=1.8$, $H_0=3$ Oe. (c) Same as (a) except $H_1=4.5$ Oe. (d) Solid lines: Same as (b), except $H_1=4.5$ Oe; for $n=10$ the dashed line is that predicted for $\beta=1$, and does not fit the data.

$H_1 = H^*$. We observe two peaks, the lower one at $H_1 = 15$ Oe and the much higher one at $H_1 = 250$ Oe, which we ascribe to inter- and intragranular contributions, respectively. The lower peak was found to be independent of frequency in the range $85-10^4$ Hz, but apparatus limitations of $|H_1|$ at high frequencies did not allow a similar conclusion for the high peak. Figure 1(b) is a plot of μ' vs $\log_{10} H_1$ which also shows, but less distinctly, two components: (i) the flat plateau region $15 \lesssim H_1 \lesssim 80$ Oe, due to full vortex penetration of the intergranular component, corresponds to $\mu'_{\rm tot} = 0.17$ which we take to be $\mu_{\rm eff}$ for this component; (ii) a steeply rising second region which does not reach a plateau (corresponding to $\mu'_g \rightarrow \mu'_{\rm tot}$) owing to insufficient H_1 field availability. Next, the same $YBa_2Cu_3O_7$ sintered bar material was ground in an agate mortar to a fine powder (sample No. 3); optical microscope examination showed grains of sizes $1 \lesssim R_g \lesssim 60$ μm, with rough average $\bar{R}_g \sim 10$ μm. To further isolate the grains, one volume of this powder was mixed with one volume of 1 μm grit Al_2O_3 powder and one volume of 0.1 μm grit Al_2O_3 powder (sample No. 4). Both powder samples display similar behavior. The data in Fig. 1(c) for sample 4, μ'' vs $\log_{10} H_1$, show essentially no evidence for the lower peak, although the high peak at $H_1 = 250$ Oe remains, and is ascribed to the collective intragranular supercurrents within individual grains. We conclude that powdered samples do not allow significant circular shielding currents on the scale of R, but only on the scale of R_g, thus invalidating the above critical-state model for the intergranular component.

To select the best-fitting values of β and H_0 for the intergranular component it was found useful to take additional measurements of $\tilde{\mu}$ vs $\log_{10} H_1$ for the sintered rod sample for various values of $H_{\rm dc}$. In Fig. 1(d), for $H_{\rm dc} = 10.2$ Oe, the low field μ'' peak splits into two, at 7.5 and at 25 Oe ($\approx H_{\rm dc} + H^*$). For the parameter values $\beta = 1.8 \pm 0.2$ and $H_0 = 3 \pm 1$ Oe our model gives quite reasonable predictions for μ' and μ'' shown as solid lines in Figs. 1(a)-1(d). These parameters correspond to $\alpha' \approx 600$, to a pinning force density $\alpha = 250$ Oe^{2}cm, and to a critical current density $J_c(H = H^*/2) = 80$ A/cm^2, which decreases as $J_c(H) \sim H^{-1.8}$. The original Bean model predicts $J_c = cH^*/4\pi R = 78$ A/cm^2 (independent of H). We conclude that in the region $0 < H_a \lesssim 50$ Oe, $\tilde{\mu}_{\rm tot}$ is dominated by the intergranular component.

To further test the model for a sintered rod from the same batch we measured the harmonic power spectrum $P_n(H_{\rm dc})$ shown in Fig. 2(a) for $H_1 = 13.5$ Oe and in Fig. 2(c) for $H_1 = 4.5$ Oe, obtained by slowly scanning $-25 \leq H_{\rm dc} \leq 25$ Oe. After several scan cycles, $P_n(H_{\rm dc})$ shows very reproducible dips with a small hysteresis. For $H_{\rm dc} = 0$ only odd harmonics are observed; even a very small dc field ($H_{\rm dc} > 10^{-3}$ Oe) breaks the symmetry and all harmonics are then observed; this is explicable by the zero-order model[6] and the BAK model.[8,10] However, the detailed shapes of $P_n(H_{\rm dc})$ have not previously been satisfactorily explained. The solid lines in Figs. 2(b) and 2(d) show the predicted results from our modified critical-state model using the same parameters for the intergranular component as for Fig. 1. All features are rather well explained (except for the small hysteresis which requires a further modification of our model). We find that $P_n(H_{\rm dc})$ is quite sensitive to $J_c(H)$: in Fig. 2(d), $n = 10$, the dashed line is predicted by changing $\beta = 1.8$ to $\beta = 1$, corresponding to the BAK model;[8,10] it fails to explain the two dips at $H_{\rm dc} = \pm 20$ Oe. In fact, it fails to predict any power dips for $H_{\rm dc} \geq H_1$, but these are observed in Fig. 2(c). More generally, the parameter $\beta = 1$ systematically fails to explain detailed data for $\tilde{\chi}_{\rm ac}$ for the same sintered sample, which require $\beta \approx 2$ in the model.[14] We measured the dependence of P_n on H_1 for odd harmonics at $H_{\rm dc} = 0$, finding this behavior: $P_n(H_1) \propto H_1^6$ for $n = 3,5$ for $2 < H_1 < 10$ Oe; at $H_1 \approx H^* = 13.5$ Oe saturation begins, and a plot of $P_n(H_1)$ becomes flat for $22 < H_1 < 36$ Oe, the maximum available field at 10.5 kHz. For higher harmonics ($n = 13,15$) kinks in $P_n(H_1)$ develop for $15 < H_1 < 30$ Oe, and saturate at higher fields. This overall behavior is predicted by the above intergranular model.

Turning now to modeling the intragranular component $\tilde{\mu}_g$ for the sintered rod sample No. 2, the dashed lines in Figs. 1(a)-1(d) represent that predicted by the above model with parameters $\beta_g = 1$, $H_{0g} = 5$ Oe, $\mu_{{\rm eff}\,g} = 1 - \mu_{\rm eff} = 0.83$; this value of $\mu_{{\rm eff}\,g}$ is to be expected for the density of our sample.[15] The predicted values of μ''_g have been reduced by a factor of 3 to better compare the shapes to the data. Using the well-measured value $H_g^* = 250$ Oe and the rough value $\bar{R}_g = 10$ μm, the parameters correspond to a pinning force density $\alpha_g = 2 \times 10^6$ Oe^{2}cm and a critical current density $J_c(H_g^*/2) = 2 \times 10^5$ A/cm^2. We have no simple explanation of why the predicted $\mu''_g(H_1)$ shows a sharper and higher peak than the data, but note that the actual grains are not long thin cylinders, as the 2D model assumes, but rather more cubical in proportions, and are randomly oriented and anisotropic, a problem too complex to treat here.

Powdered samples. Samples No. 3 and No. 4 yield harmonic power spectra $P_n(H_{\rm dc})$ closely resembling that reported earlier[19] for a different powdered sample: a smooth, featureless set of almost periodic dips spaced by $\Delta H_{\rm dc} \approx H_1/n$, not explicable, nor expected to be, by the above modified critical-state model for the intergranular component. We observe $P_n(H_1) \propto H_1^{1.5}$, and very little saturation, in sharp contrast to that for sintered rods. For $H_1 = 13.5$ Oe, P_3 for the powder sample (No. 1) is 32 dB *less* than that for the sintered rod; however, P_{15} is *greater* by 17 dB than the rod's. We found that the above critical-state model and parameters for the *intragranular* component would not fit the harmonic power data, but by assuming $H_0 \approx 30$ to 100 Oe and arbitrarily setting $\mu''_n \ll \mu'_n$, we were able to obtain a moderate fit. Nevertheless, the origin of the harmonic spectra for powders remains unclear and could possibly be due to a third region, *inside* the grains, e.g., twin boundaries, easily penetrated by low fields.

We have shown, for both $\tilde{\mu}_1(H_1)$ and harmonic power measurements, $P_n(H_{\rm dc})$ for a sintered cylinder of $YBa_2Cu_3O_7$, that the behavior is quantitatively described by a modified intergranular critical-state model in which $J_c(H) \sim H^{-2}$, for $H \lesssim 50$ Oe. For $H \gtrsim 100$ Oe the behavior is dominated by intragranular effects, less well understood.

This work was supported in part by the Director, Office of Energy Research, Office of Basic Energy Sciences, and Materials Sciences Division of the U.S. Department of Energy under Contract No. DE-AC03-76SF00098; the Office of Naval Research under Contract No. N00014-86-K-0154.

[1]R. B. Goldfarb *et al.*, Cryogenics **27**, 475 (1987); A. Raboutou *et al.*, Europhys. Lett. **4**, 1321 (1987); D. X. Chen *et al.*, J. Appl. Phys. **63**, 980 (1988).

[2]B. Renker *et al.*, Z. Phys. B **67**, 1 (1987).

[3]J. F. Kwak *et al.*, in *Proceedings of the International Workshop on Novel Mechanisms of Superconductivity, Berkeley, June, 1987,* edited by S. A. Wolf and V. Z. Kresin (Plenum, New York, 1987), p. 983; R. L. Peterson and J. W. Ekin, Phys. Rev. B **37**, 9848 (1988).

[4]K. W. Blazey *et al.*, Phys. Rev. B **36**, 7241 (1987); K. Khachaturyan *et al.*, *ibid.* **36**, 8309 (1987); R. Durny *et al.*, *ibid.* **36**, 2361 (1987); E. J. Pakulis *et al.*, Physica C **153–155**, 510 (1988); S. H. Glarum, J. H. Marshall, and L. F. Schneemeyer, Phys. Rev. B **37**, 7491 (1988).

[5]Carson D. Jeffries *et al.*, Phys. Rev. B **37**, 9840 (1988); Q. Harry Lam and Carson D. Jeffries, *ibid.* **39**, 4772 (1989).

[6]C. D. Jeffries *et al.*, Phys. Rev. B **39**, 11 526 (1989).

[7]A. Shaulov and D. Dorman, Appl. Phys. Lett. **53**, 2680 (1988).

[8]K.-H. Müller, J. C. Macfarlane, and R. Driver, Physica C **158**, 366 (1989).

[9]K.-H. Müller, J. C. Macfarlane, and R. Driver, Physica C **158**, 69 (1989); K.-H. Müller, *ibid.* **159**, 717 (1989).

[10]L. Ji *et al.*, Phys. Rev. B **40**, 10936 (1989).

[11]C. P. Bean, Phys. Rev. Lett. **8**, 250 (1962); Rev. Mod. Phys. **36**, 31 (1964).

[12]Y. B. Kim, C. F. Hempstead, and A. R. Strnad, Phys. Rev. **129**, 528 (1963); P. W. Anderson and Y. B. Kim, Rev. Mod. Phys. **36**, 39 (1964).

[13]Briefly reported by Q. H. Lam and C. D. Jeffries, Bull. Am. Phys. Soc. **35**, 339 (1990).

[14]Youngtae Kim and C. D. Jeffries, Bull. Am. Phys. Soc. **35**, 338 (1990); Youngtae Kim, Q. Harry Lam, and C. D. Jeffries (unpublished).

[15]$YBa_2Cu_3O_7$ sintered bar provided by National Superconductor, Inc.; $T_c = 92.5$ K, measured from onset of χ'_{ac}; measured density $\rho = 5.46 \pm 0.05$ g/cm^3, which is 0.85 of the density $\rho = 6.38$ g/cm^3 computed from x-ray structure [see, C. P. Poole, Jr., T. Datta, and H. A. Farach, *Copper Oxide Superconductors* (Wiley, New York, 1988)]. Fabricated from this bar: a cylinder of diameter 2.5 mm, length 19 mm (sample No. 1); a cylinder of diameter 3.1 mm, length 23 mm (sample No. 2); a powdered sample (No. 3); and a powdered sample diluted with Al_2O_3 powder (sample No. 4).

[16]J. R. Clem, Physica C **153–155**, 50 (1988).

[17]H. Küpfer *et al.*, Cryogenics **28**, 650 (1988).

[18]V. Calzona *et al.*, Physica C **157**, 425 (1989).

[19]Reference 6, Figs. 5 and 6.